Journal of the Association of Arab Universities for Basic and Applied Sciences (2015) 17, 66–72

University of Bahrain
Journal of the Association of Arab Universities for Basic and Applied Sciences
www.elsevier.com/locate/jaaubas
www.sciencedirect.com

المعالجة الحرارية المثلى للأقطاب الضوئية المصنوعة من حبيبات أكسيد الزنك النانوية للحصول على افضل اداء للخلايا الشمسية الصبغية

Amal Al-Kahlout

Department of Physics, Al-Azhar University-Gaza – AUG, P.O. Box 1277, Gaza-Strip, Palestine.

الملخص:

تؤثر درجة الحرارة التي يعالج بها القطب الضوئي المستخدم في الخلايا الشمسية الصبغية بشكل فعال وملحوظ على أداء تلك الخلايا. وفي هذا الاطار تم تحضير أقطاب مختلفة من حبيبات أكسيد الزنك النانوية على شريحة زجاجية مطلية بمادة موصلة ومن ثم معالجتها عند درجات حرارة مختلفة تتراوح ما بين 200 و 500 درجة سيليزية. وبدراسة الخصائص الحرارية للعجينة المستخدمة في صناعة الأقطاب باستخدام تقنية (DTA/TG)، تم الكشف عن عدم حدوث أي تغيرات عند درجات حرارة أعلى من 350 درجة سليزية. لقد تم دراسة الخصائص الكهربائية للخلايا الشمسية الصبغية المحضرة عند درجات الحرارة المختلفة من خلال دراسة خصائص العلاقة بين التيار وفرق الجهد وقياس مطيافية الممانعة الكهروكيميائية. النتائج أظهرت بأن المساحة السطحية ومدى التصاق المادة الصبغية بحبيبات أكسيد الزنك في القطب الضوئي تزداد بزيادة درجة الحرارة التي تعالج عندها الأقطاب وصولاً إلى 350 درجة سليزية. في حين أن زيادة درجة حرارة معالجة الاقطاب اعلى من 400 درجة سليزية أدى إلى نقص في كثافة التيار الناتج عن الخلية الشمسية الصبغية مما اثبت أن هناك تأثير لدرجة الحرارة على أداء هذا النوع من الخلايا. لقد بينت الدراسة بانه عند درجة تسخين مساوية الى 400 درجة سليزية، قد تحققت أعلى قيمة لكثافة التيار الكهربائي بحيث كانت $15.6\ mA/cm^2$ وفرق جهد الدائرة المفتوحة كان 0.55V والكفائة كانت 3.01% .

Journal of the Association of Arab Universities for Basic and Applied Sciences (2015) **17**, 66–72

University of Bahrain

Journal of the Association of Arab Universities for Basic and Applied Sciences

www.elsevier.com/locate/jaaubas
www.sciencedirect.com

ORIGINAL ARTICLE

Thermal treatment optimization of ZnO nanoparticles-photoelectrodes for high photovoltaic performance of dye-sensitized solar cells

Amal Al-Kahlout *

Department of Physics, Al-Azhar University-Gaza – AUG, P.O. Box 1277, Gaza-Strip, Palestine

Received 1 July 2013; revised 13 January 2014; accepted 11 February 2014
Available online 17 March 2014

KEYWORDS

ZnO nanoparticles;
Dye sensitized solar cell;
Annealing temperature

Abstract Annealing temperature has pronounced effect on DSSC performance. ZnO nanoparticles photoelectrodes were prepared on FTO glass and annealed at different temperatures in the range 200–500 °C. The thermal properties of the paste were studied using DTA/TG technique which revealed that no changes are expected at temperatures higher than 350 °C. Electrical properties of the DSSCs using ZnO nanoparticles photoelectrodes annealed at different temperatures were studied using *I–V* characteristic and electrochemical impedance spectroscopy (EIS). The surface area and dye loading increased as the annealing temperature increased up to 350 °C. The electrical properties are found to be dependent on the photoelectrode annealing temperature. Annealing temperatures higher than 400 °C resulted in a decrease in current density. The highest value of current density *I*sc (15.6 mA/cm^2), open circuit potential Voc (0.55 V) and efficiency (3.01%) is achieved at annealing temperature of 400 °C.

1. Introduction

Photovoltaic technology provides clean and renewable energy that can reduce the world's dependency on fossil fuels. Dye sensitized solar cell (DSSC) is one of the choices because of its low cost fabrication and potential application for flexible devices (Ribeiro et al., 2009). DSSC is a new type of metal–oxide wide-band-gap solar cells. It composes of dye-modified wide band gap semiconductor photoelectrode, a counter electrode and an electrolyte containing a redox (Raksa et al., 2009). A common photoelectrode material in DSSCs is TiO_2 nanoparticle film on transparent conducting oxide (TCO) layers (Chiba et al., 2006). The popularity of this material is due to its adequate surface area and chemical affinity for dye adsorption as well as its suitable energy band potential for charge transfer with dye and electrolytes (Bandara et al., 2005).

ZnO-based DSSCs have been exploited as an alternative to TiO_2 based one. ZnO nanostructures have shown the unique multifunctional properties with high exciton binding energy (60 meV), low resistivity, non-toxicity, high transparency in the visible range and high light trapping characteristics (Caglar et al., 2009). External quantum efficiencies using purely ZnO as the active material has generally been below 3% but with

* Address: Department of Physics, Al-Azhar University-Gaza – AUG, P.O. Box 1277, Gaza-Strip, Palestine. Tel.: +970 599369536.
E-mail address: dramalkahlout@yahoo.com.

Peer review under responsibility of University of Bahrain.

1815-3852 © 2014 Production and hosting by Elsevier B.V. on behalf of University of Bahrain.
http://dx.doi.org/10.1016/j.jaubas.2014.02.004

some dye-sensitized solar cells using liquid electrolytes it was reported to be above 5%. The highest reported efficiencies to date were from combinational structures at 7.07% for ZnO nanosheets with TiO_2 nanoparticulate coating which is approaching the ~11% efficiency level of TiO_2 nanoparticle-based DSSCs (Chiba et al., 2006; Keis et al., 2002; Loh and Dunn, 2012).

ZnO-based DSSCs are still challenging and need to be studied further so that their photovoltaic properties can be improved. For example, suitable electrolyte and dye materials need to be developed, and the fabrication parameters and design of the nanostructure need to be optimized, which is essential for maximizing the energy conversion efficiency (Kakiuchi et al., 2006; Rao and Dutta, 2008). The effect of the morphology, thickness and presence of aggregates of nanostructured ZnO films on the efficiency of dye-sensitized solar cells was studied by Giannouli and Spiliopoulou (2012) while Chang et al. (2012) reported the optimization of dye adsorption time and film thickness for efficient ZnO dye-sensitized solar cells with high at-rest stability.

ZnO dye-sensitized solar cells (DSSCs) with different photoelectrode nanostructures were studied. The main nanostructural forms of ZnO developed during the past several decades include nanoparticles, nanorods, nanotubes, nanobelts, nanosheets and nanotips. Considerable efforts have been devoted to the synthesis of one dimensional structures such as rods or wires (Lai et al., 2011; Kang et al., 2008; Jennings et al., 2008; Xu et al., 2010) and nanotubes (NTs) (Martinson et al., 2007; Yang et al., 2012) to significantly enhance the electron transport speed in the photoelectrode as they provide a direct conduction pathway for the rapid collection of photo generated electrons. Yang et al. (2009) studied the effects of ZnO and TiO_2 buffer layers on ZnO nanowire-based dye-sensitized solar cells (DSSCs). Raksa et al., 2009 studied the effect of CuO layer as a barrier layer toward power conversion characteristics.

Due to the instability of ZnO in acidic dyes (Pugliese et al., 2013), alternative type dyes provide a new pathway for improving the performance of ZnO dye-sensitized solar cells. Various types of dyes include heptamethine-cyanine dyes for absorption in the red/near-infrared (IR) region (Matsui et al., 2005), and unsymmetrical squaraine dyes with deoxycholic acid, which increases photo-voltage and photocurrent by suppressing electron back transport (Hara et al., 2003). Wu et al., 2007 reported that a mercurochrome ($C_{20}H_8Br_2HgNa_2O$) sensitizer is more suitable than the currently used Ru(dcbpy)2(NCS)2 (N3) dye for ZnO nanorod-based DSSCs. Guillén et al., 2008 used Eosin Y, Eosin B and Mercurochrome to compare their performance to that of the more common N719 dye and reported that these dyes efficiently sensitize commercial ZnO nanopowder and yield efficiencies that are very competitive with respect to those provided by N719. The annealing temperature of photoelectrode layer is critical for improving the energy conversion efficiency of ZnO-based DSSCs (Noh et al., 2008). It is well known that annealing removes impurities and improves crystallinity of ZnO nanoparticles without influencing its Wurtzite phase (Matsui et al., 2005). The improved crystallinity and reduced grain boundary regions improve charge transport but they affect the solar cell efficiency in opposite ways. The surface area of the semiconductor decreases with increasing grain growth leading to lower dye adsorption in DSSC's which results in lower charge generation efficiency. This finding illustrates the need for extensive studies on optimization of ZnO photoelectrode heating temperature for improving ZnO-based DSSC performance.

In this work, the effect of the annealing temperature of ZnO nanoparticle layers on the performance of DSSCs is investigated. The annealing temperature's influence on the charge transport property of ZnO-based DSSCs is studied through electrochemical measurements and electrochemical impedance spectroscopy (EIS) analysis.

2. Experimental details

2.1. Nanopowder synthesis

ZnO nanoparticles were prepared using a method described in our previous work (Alkahlout, 2012). A 0.5 M/L methanolic sol. of zinc acetate dihydrate, reagent $Zn(CH_3COO)_2.2H_2O$ (ACROS) was left under stirring overnight. A 3 M aqueous solution of sodium hydroxide (NaOH) was added drop wise to the solution under vigorous stirring forming a white suspension that was left under stirring for 12 h at room temperature. The pH value of the solution, measured using a pH meter, METTLER TOLEDO InLab Expert Pro, was adjusted to 12. The white slurry was washed with extra methanol to remove the precursor material and dried in air at 100 °C for 12 h. The powder was grinded using a hammer mill to reduce the size of the agglomerates until obtaining a fine powder.

2.2. Paste, layer deposition and sensitization

2 g of ZnO nanopowder was wetted with 0.2 g of polyethylene glycol (PEG 400). The obtained paste was dispersed mechanically in mortar until a very soft uniform paste was obtained. A 5 mL of ethanol was then added to the paste to obtain a suitable viscosity for the coating preparation.

ZnO paste was deposited on fluorine-doped SnO_2-(FTO)-coated glass substrates using the "doctor blade" technique to form 0.5×0.5 cm layers. The layers were dried at 100 °C for one hour, followed by heating in air at various temperatures ranging from 200 to 500 °C.

The dye sensitization was carried out by dipping the electrodes into a solution of 0.5 mM of Ruthenium535 (Solaronix), known as N3, in ethanol for a few hours. The layers were immersed in the dye solution while they were still warm to enhance the coloration and to prevent the capillary condensation of water vapor from ambient air inside the nanopores of the film. The thickness of the layers was measured using a Profilometer, P10 surface Profiler, TENCOR.

2.3. Cell assembly and characterization

To assemble the solar cells, a Pt-coated conducting glass was placed on the ZnO photoelectrode separated by a 10 μm thin membrane spacer. The assembled cell was then clipped together. The electrolyte, consisted of a mixture of acetonitrile (ACN, C_2H_3N from Sigma–Aldrich) and propylene carbonate with a ratio of 20:80 vol.% respectively, and a redox system based on the iodine/triiodide system, 0.5 M lithium iodide anhydrous LiI (Flucka Chemika) and 0.05 M iodine I_2 (Flucka

Chemika), were injected into the open cell from the edges by capillarity.

The morphologies of photoelectrode surfaces were characterized by scanning electron microscopy (SEM, JEOL JSM-7000), and the BET surface areas and pore size distributions of the layers were determined using a Brunauer–Emmett–Teller (BET, Quantachrome NOVA 4200e).

To measure the adsorbed amount of N3 dye on the ZnO films, the dye was desorbed by immersing the dye sensitized films in an 0.1 M NaOH solution in water and ethanol (with volume ratio of 1:1). An ultraviolet–visible–near-infrared spectrophotometer (UV–VIS–NIR, Perkin Elmer Lambda 900) was employed to measure the dye concentrations of the desorbed-dye solutions.

The thermal properties of the paste have been determined by differential thermal analysis and thermal gravimetry analysis (DTA/TG) using a Netzsch STA 449 C Jupiter instrument. 33.3 mg of the paste was heated in synthetic air in an Al_2O_3 crucible up to 500 °C at a heating rate of 2 K/min.

Photovoltaic properties of solar cells were characterized using an EG&G Princeton Applied Research Potentiostat/Galvanostat model 273. The illumination source was a 450 W Xenon lamp from Mueller Electronik Optik with an intensity of 200,000 Lux as measured by a light Meter Voltcraft LX-11008. As the performance of DSSC is greatly influenced by many factors, many sets of samples were tested separately and for each annealing temperature, the cell was tested many times (more than 10 times) to ensure that the obtained results are reproducible and valid.

Electrochemical impedance spectroscopy (EIS) was performed using a Solartron 1287A coupling with a Solartron 1260FRA/impedance analyzer to investigate the electronic and ionic processes in the DSSCs.

3. Results and discussions

3.1. Structure and morphology of the coatings

The XRD data of powder synthesized at room temperature is shown in Fig. 1. The pattern shows that the powder is highly crystalline and that its structure is in accordance with the typical Wurtzite hexagonal structure (JCPDS No. 0036-1451 WL 15406 Hexagonal-03 24982). The XRD data of the coatings (not shown) is not different from those of the corresponding powder as they also show the Wurtzite hexagonal structure. The crystallite size calculated for the (1 0 0), (0 0 2) and (1 0 1) peaks is about 20 nm. Neither changes in the structural phase nor the crystallinity are observed by increasing the heating temperature because the layers were deposited from already highly crystalline ZnO nanoparticles. Same conclusion is reported by Teesetsopon et al. (2012).

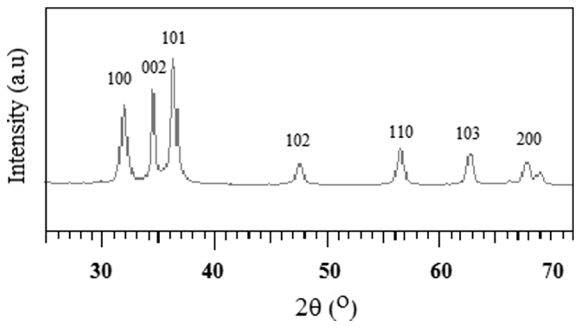

Figure 1 XRD pattern of the ZnO layer deposited on K-glass and sintered at 400 °C. The peaks refer to the Wurtzite hexagonal structure in the reference data (JCPDS No. 0036–1451).

SEM pictures of ZnO layers sintered at different temperatures are shown in Fig. 2. The thicknesses of the films are found to be about 15 μm. All samples, regardless of heating temperatures, consist of nanoparticles ~30 nm in thickness (see inset of the figure). Clearly, the top surface of the films has a macro porous structure. Image of layer heated at 200 °C (Fig. 2a) shows nonhomogeneous aggregates with loosely packed nanoparticles dispersed in organic medium. The layers sintered at 300 and 400 °C (Fig. 2b and c) show a homogeneous distribution of closely packed, aggregated nanoparticles. Sintering temperature of the layer is found to affect the particles size and porosity of the layers where sintering the layer at high temperatures helps the growth of the oxide particles reducing the grain boundary (Fig. 2d). The decrease in layer porosity may be attributed to degradation and removal of the organic species of the binder used in preparing the paste. The particles growth and reduced grain boundary regions affect the solar cell efficiency in two different ways. The surface area of the semiconductor is reduced with increased grain growth leading to lower dye adsorption in DSSC resulting in lower light harvesting. On the other hand, reduction of dangling bonds due to reduced grain boundaries improves charge collection efficiency. Hence, optimization of the grain growth and the reduction of dangling bonds are required to improve DSSC efficiencies. Teesetsopon et al. (2012) reported that sintering of ZnO nanoparticles occurs as annealing temperature was increased from 350 to 450 °C which was attributed to the mass transport between connecting particles.

3.2. Thermal properties of ZnO paste (DTA/TG)

Typical differential thermal analysis and thermal gravimetry spectra obtained for a ZnO paste prepared as described above are shown in Fig. 3. The curve shows three distinct features. The first is a well defined endothermic peak observed in the temperature range below 100 °C with its maximum at 50 °C. It is accompanied by a mass loss of about 5.5 wt.%. This endothermic peak indicates essentially the evolution and removal of physically adsorbed H_2O due to drying of the paste. The second feature of the DTA curve is strong exothermic peak in the temperature range 170–350 °C with maximum at 257 °C. This feature is accompanied by the main mass loss (about 35 wt.%) which is attributed to the decomposing and combustion of PEG_{400} used in preparing the paste. The final feature is a small peak centered at 292.5 °C which is due to the condensation of the layer. A net weight loss of 40 wt% accompanied the whole heating process, which is almost the same concentration as the PEG_{400} used in the paste. No further changes are observed at temperatures higher than 350 °C. This indicates that decompositions and combustions of the organic bonds of PEG and the transformation into ZnO are complete at this temperature.

3.3. Dye loading

The absorption spectra in the visible region of samples heated at different temperatures are shown in Fig. 4. The absorption

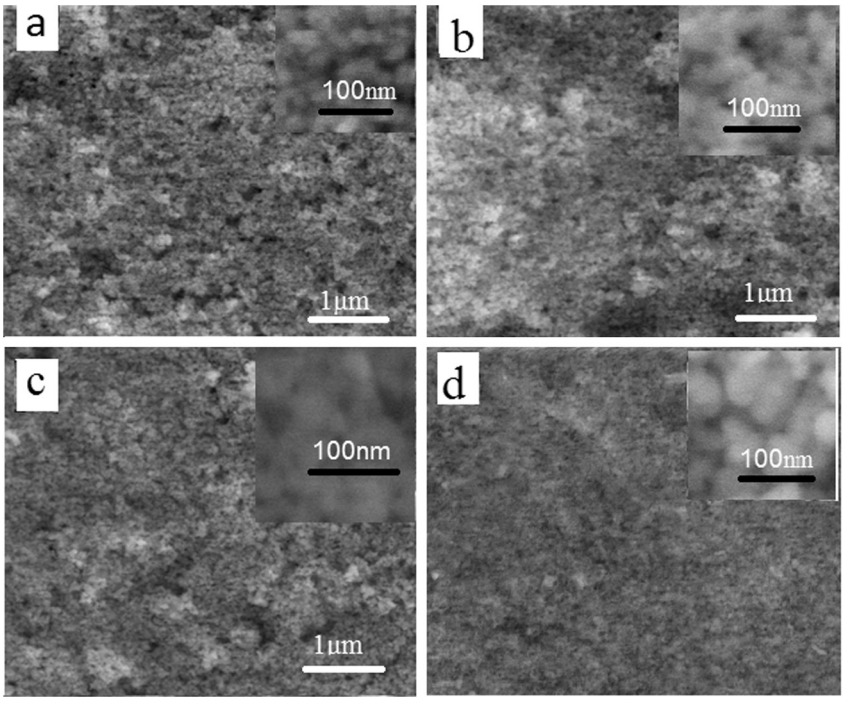

Figure 2 SEM surface images of ZnO nanoparticles annealed at 100 °C (a), 200 °C (b), 300 °C (c) and 400 °C (d).

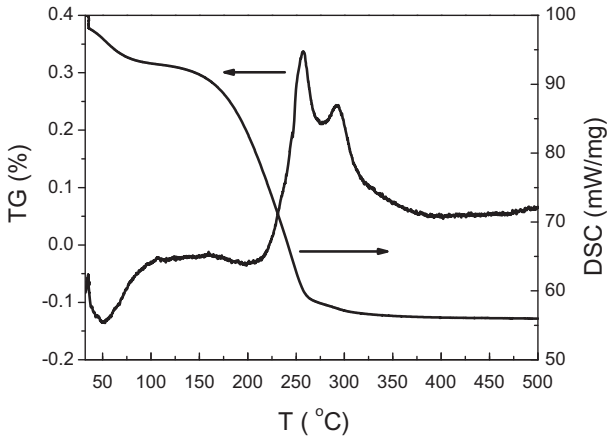

Figure 3 DTA/TG thermal analysis of a ZnO paste, heating rate 2 K/min in synthetic air.

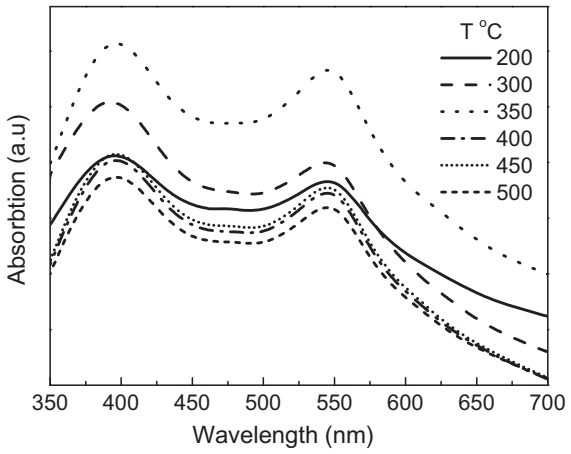

Figure 4 UV–VIS absorbance of dye de-adsorped from ZnO photoelectrodes annealed at different temperatures.

of the samples increases by increasing the heating temperature from 200 up to 350 °C, then decreases again at higher temperatures. Based on the experimental data shown in the UV–Vis absorption spectra, the amount of dye loaded on each layer is estimated to be 1.5×10^{-7}, 2.5×10^{-7}, and 1.4×10^{-7} mol/cm^2 for the samples treated at 200, 350 and 500 °C, respectively. This was expected as a result of the changes in surface morphology. As shown in Fig. 2a, the structure of samples sintered at low temperature is rough and porous but in spite of that the layer content of the organic species is high which prevents good adsorption of dye molecules on the surface of the oxide nanoparticles which explains the low amounts of loaded dye on photoelectrode sintered at this temperature. By increasing the heating temperature the organics are consumed and particles are expected to have larger surface area (Fig. 2b), which is more convenient for dye loading where the highest amount of loaded dye is found for layers sintered at 350 °C. Layers which are sintered at temperature higher than 350 °C have more compact structure with less pores (Fig. 2c and d) and lower surface area when compared with layers sintered at lower temperatures which lower the amount of loaded dye leading to low absorption of these layers. These results indicate that 350 °C is the optimum temperature for getting the highest amount of dye loading. The increase in dye loading could result in a better light harvesting and a higher photocurrent conversion efficiency of the device, which is obvious from the results in Table 1.

Table 1 ZnO–DSSC performance with photoelectrodes annealed at different temperatures.

Temperature (°C)	Voc (mv)	*I*sc (mA/cm^2)	Efficiency (%)	FF
200	545	4.42	1.07	0.44419
300	544	12.51	2.02	0.29682
350	550	12.87	2.38	0.33623
400	552	15.66	3.01	0.34821
450	554	13.38	2.26	0.30489
500	573	8.64	1.47	0.29693

3.4. BET surface area

The nitrogen adsorption/desorption isotherms at 77 K and BET surface area of samples heated at different temperatures starting from 200 to 500 °C are presented in Fig. 5a and b. All samples have similarly shaped hysteretic behaviors. The isotherm of the sample heated at 300 °C has the largest inflection for the nitrogen adsorption volume at $P/P\text{o} = 0.9$. The value decreased by increasing the heating temperature. This result reveals that samples heated at 300 °C are more porous than samples heated at other temperatures.

The determined BET surface area was found to increase from 18 to 26.2 m^2/g by increasing annealing temperature from 200 up to 300 °C. It then started to decrease by increasing the annealing temperature to reach 15.08 m^2/g at 500 °C. Large surface area implies large exposed active region for the electrochemical reaction, which means that large amount of dye is loaded on ZnO nanoparticles. This is in agreement with the result obtained from dye loading in Section 3.3 where the dye loading increases by increasing temperature up to 350 °C then started to decrease again by increasing the sintering temperature due to particle growth which reduces the surface area leading in turn to decrease in dye loading.

3.5. Electrochemical characterization

Current–Voltage (*I–V*) characteristics under light illumination is used to determine the electrical properties of DSSC, namely, open circuit voltage (Voc), short circuit current density (Jsc) and cell efficiency (η). Fig. 6 shows the photocurrent–voltage characteristics of ZnO nanoparticle DSSC solar cells with photoelectrodes annealed at different temperatures. From the figure it is seen that increasing heating temperature of the photoelectrode layers from 200 to 400 °C improved both the photocurrent density and the open circuit voltage where Jsc increases from 4.42 mA/cm^2 at 200 °C to reach a maximum value of 15.66 mA/cm^2 at 400 °C with an increase in the efficiency from 1.07% to 3.01%. Photoelectrodes annealed at low temperature contain many impurity sites and imperfections due to residual organics used in paste preparation. These defects and impurities lower dye adsorption due to lack in surface area available for dye loading. By increasing the annealing temperature the organics are burned out and the surface area of ZnO nanoparticles available to dye loading increases up to 350 °C (see Section 3.3). This increases light harvesting at the photoelectrode which in turn increases short circuit current density. By further increasing annealing temperature to 400 °C, grain growth occurs resulting in better connection between photoelectrode particles. The obtained higher current density is thus attributed to a better charge collection caused by lowering charge scattering at the grain boundary interfaces of the ZnO nanoparticles. At this temperature (400 °C) the highest current density is obtained. By increasing the heating temperature higher than 400 °C the current density decreases to reach a value of 1.47 mA/cm^2 at 500 °C with efficiency of 1.47%. Obviously, the considerable decrease of the short-circuit current density Jsc for layers annealed at temperatures higher than 400 °C is attributed to the decrease of light harvesting of the ZnO photoelectrode due to the decrease in surface areas of the particles provided for dye adsorption. This is confirmed through measuring the dye loading level (see Section 3.3) and BET surface area (Section 3.4). The main changes of the efficiency of photoelectrodes heated at different temperatures are coming from the changes of the photocurrent density, while a minimal change of the open circuit voltage is observed where it increases from 545 mv at 200 °C to 573 mv at 500 °C. For photoelectrodes heated at low temperature the injected electrons from dye to conduction band of ZnO recombine in the defect sites quickly and hence the electron density in the conduction band of the ZnO becomes less which results in lower Voc. By increasing the annealing temperature, defects and impurities are removed and Voc increases. In addition, the fill factor of the DSSC is found to be dependent on the heating temperature of ZnO photoelectrode. It increases by increasing the temperature up to 400 °C then decreases at higher temperatures. The lower FF implies that the photoelectrons in the photoelectrode are easy to back react with I_3^- in the electrolyte which will be discussed in Section 3.6.

These results are in agreement with the results reported by Teesetsopon et al. (2012) for ZnO nanoparticles–DSSC while an optimum annealing temperature of 350 °C has been obtained for the maximum ZnO nanorods-DSSC performance (Kyaw et al., 2009). It was attributed to better crystallinity and defect removal of the photoelectrode. Kao et al. (2010) studied the effect of annealing temperature on nanocrystaline ZnO–DSSC in the temperature range 100–300 °C. They attributed to the improvement in cell performance with increasing annealing temperature to the increase in pore size and surface area of ZnO improving the absorption of N3 dye onto the films.

3.6. EIS spectroscopy

Electrochemical impedance spectroscopy (EIS) is very useful to understand the inner resistance and charge transfer kinetics of DSSCs. The electron transport properties of the DSSCs with ZnO photoelectrodes annealed at different temperatures were investigated by electrochemical impedance spectra. Fig. 7 shows the Nyquist plots of the impedance data of ZnO–DSSCs at the applied bias of Voc. By analyzing the data

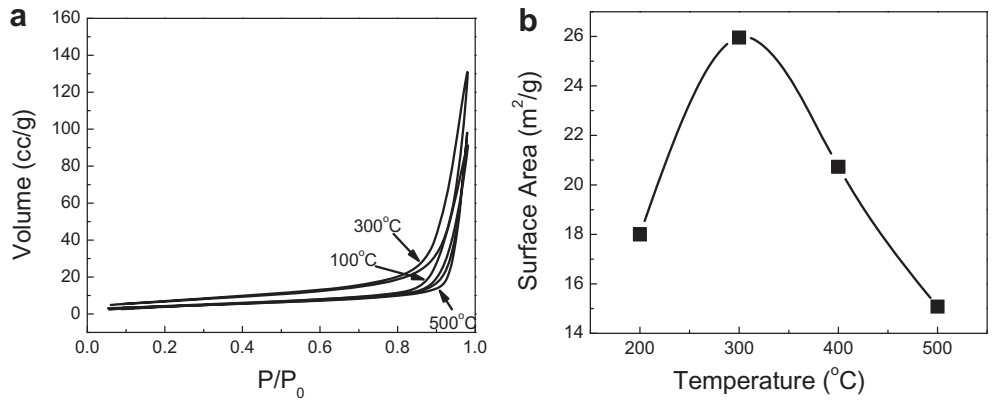

Figure 5 Adsorption–desorption isotherm using N2 at 77 K (a) and surface area (BET) (b) for ZnO nanoparticles annealed at different temperatures.

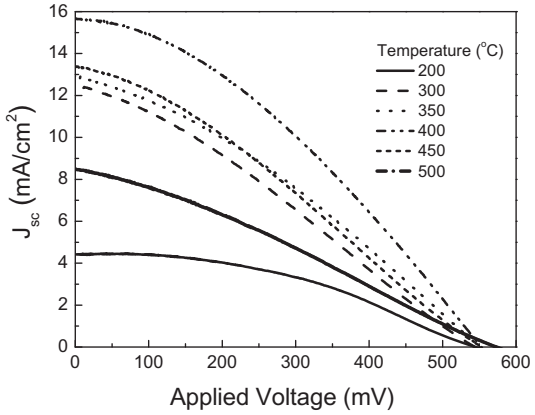

Figure 6 Current–Voltage characteristics of ZnO–DSSCs using ZnO nanoparticles photoelectrodes annealed at different temperatures.

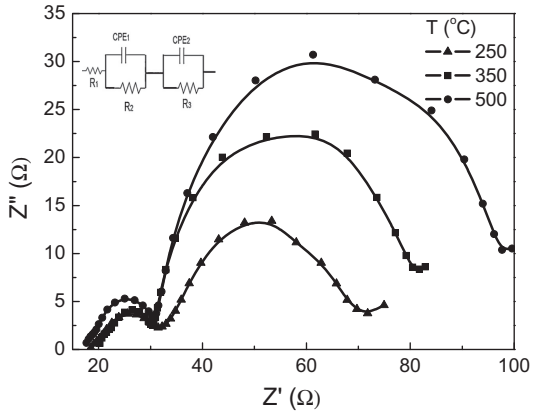

Figure 7 Nyquist plots of ZnO-DSSCs using photoelectrode annealed at different temperatures (250 °C, 350 °C and 500 °C) with equivalent circuit model used in curve fitting.

through software by Zahner the equivalent circuit that fits the results is shown in the inset of Fig. 7. According to the model proposed by Wang et al. (2005) and Al Dahoudi et al. (2012) for TiO_2 based DSSC, the impedance due to the electron transfer from the conduction band of the photoelectrode to the triiodide ions in the electrolyte is represented by a semicircle in the intermediate-frequency regime. The transport resistance is shifted to lower values for photoelectrodes heated at lower temperatures. The lifetime of each electron is estimated from the frequency of the maximum peak of the semicircle. Correspondingly, the characteristic frequency is shifted to higher values for the samples annealed at lower temperatures, suggesting the electron life time is shortened. This shift can be ascribed to a difference in the local I_3^- concentration. The low transport resistance and short lifetime of layers annealed at low temperatures are due to the high recombination rate which is attributed to the increase in penetration of the redox couples in the pores of the photoelectrode (Hsua et al., 2008) where the recombination centers are close to the surface of the nanoparticles. Kang et al. (2007) reported that a lower lifetime for a mesoporous structure is attributed to its larger surface area, which is proportional to the charge recombination between the injected electrons and the redox species where many defect states are induced by an increased surface area. Such defect states provide many pathways by which charge recombination can occur within the interfaces.

The samples annealed at higher temperatures show longer life time which may be attributed to easier electron transfer within the photoelectrodes and subsequent easier charge transfer at the photoelectrode/FTO interface due to the relatively dense structure and better connections between particles in the photoelectrodes, which are beneficial for electron transport.

4. Conclusions

The impact of annealing temperature of ZnO nanoparticles photoelectrode on the photovoltaic performance of dye-sensitized solar cell (DSSC) was studied in the temperature range 200–500 °C in order to improve its performance. Increasing the heating temperature up to 350 °C improved the dye loading through the increase in particles surface area. At temperature higher than 350 °C particles grow and the photoelectrode layer became denser which decreased the surface area and lowered the amount of loaded dye. On the other hand heating the layers at high temperature improved the charge transport due to better connection between particles. *I–V* characteristics of the DSSCs with ZnO photoelectrodes heated at different tem-

peratures showed that 400 °C is the optimum temperature where the cell performance is improved (efficiency of 3.01%) due to the high photocurrent density (15.6 mA/cm^2) facilitated with more dye adsorption and better charge transport channel with less charge recombination at FTO/ZnO/electrolyte. These results indicate that overall performance in DSSC was obtained by optimizing heating temperature.

Acknowledgements

The author would like to thank the Leibniz Institute for New Material INM-Saarbreucken. Special thanks to Dr. Peter Oliveira the head of the optics group at INM. Thanks to Dr. Koch for SEM measurements.

References

Al Dahoudi, N., Xi, J., Cao, G., 2012. Silica modification of titania nanoparticles for a dye-sensitized solar cell. Electrochimica Acta 59, 32–38.

Alkahlout, A., 2012. ZnO nanoparticles and porous coatings for dye-sensitized solar cell application: Photoelectrochemical characterization. Thin Solid Films 520, 1814–1820.

Bandara, J., Pradeep, U.W., Bandara, R.G.S.J., 2005. The role of *n–p* junction electrodes in minimizing the photovoltage in dye sensitized solar cells. Photochem. Photobiol. A Chem. 170, 373–378.

Caglar, Y., Aksoy, S., Ilican, S., Caglar, M., 2009. Crystalline structure and morphological properties of undoped and Sn doped ZnO thin films. Superlattices Microstruct 46, 469–475.

Chang, W.Ch., Lee, Ch.H., Yu, W.Ch., Lin, Ch.M., 2012. Optimization of dye adsorption time and film thickness for efficient ZnO dye-sensitized solar cells with high at-rest stability. Nanoscale Res Lett. 7, 688.

Chiba, Y., Islam, A., Komiya, R., Koide, N., Han, L., 2006. Conversion efficiency of 10.8% by a dye-sensitized solar cell using a TiO_2 electrode with high haze. Appl. Phys. Lett. 88, 223505.

Giannouli, M., Spiliopoulou, F., 2012. Effects of the morphology of nanostructured ZnO films on the efficiency of dye-sensitized solar cells. Renew. Energy 41, 115–122.

Guillén, E., Casanueva, F., Anta, J., Vega-Poot, A., Oskam, G., Alcántara, R., et al, 2008. Photovoltaic performance of nanostructured zinc oxide sensitised with xanthene dyes. J. Photoch. Photobio. A 200, 364–370.

Hara, K., Sato, T., Katoh, R., Furube, A., Ohga, Y., Shinpo, A., Suga, S., Sayama, K., Sugihara, H., Arakawa, H., 2003. Molecular design of coumarin dyes for efficient dye-sensitized solar cells. Phys. Chem. B107, 597–606.

Hsua, C., Lee, K., Huang, J., Lin, C., Lee, C., Wang, L., Tsai, S., Hu, K., 2008. EIS analysis on low temperature fabrication of TiO_2 porous films for dye-sensitized solar cells. Electrochim. Acta 53, 7514–7522.

Jennings, J.R., Ghicov, A., Peter, L.M., Schmuki, P., Walker, A.B., 2008. Dye-sensitized solar cells based on oriented TiO_2 nanotube arrays: transport, trapping, and transfer of electrons. J. Am. Chem. Soc. 130, 13364–13372.

Kakiuchi, K., Hosono, E., Fujihara, S., 2006. Enhanced photoelectrochemical performance of ZnO electrodes sensitized with N-719. J. Photochem. Photobiol. A Chem. 179, 81–86.

Kang, S.H., Kim, J., Sung, Y., 2007. Role of surface state on the electron flow in modified TiO_2 film incorporating carbon powder for a dye-sensitized solar cell. Electrochima Acta 52, 5242–5250.

Kang, S.H., Chio, S.-H., Kang, M.-S., Kim, J.-Y., Kim, H.-S., Hyeon, T., Sung, Y.-E., 2008. Nanorod-based dye-sensitized solar cells with improved charge collection efficiency. Adv. Mater. 20, 54–58.

Kao, M.C., Chen, H.Z., Young, S.L., 2010. Effects of preannealing temperature of ZnO thin films on the performance of dye-sensitized solar cells. Appl. Phys. A-Mater. 98, 595–599.

Keis, K., Magnusson, E., Lindstrom, H., Lindquist, S.E., Hagfeldt, A., 2002. A 5% efficient photoelectrochemical solar cell based on nanostructured ZnO electrodes. Sol. Energy Mater. Sol. Cells 73, 51–58.

Kyaw, H.H., Bora, T., Dutta, J., 2009. Nanomaterials for health, energy and environment, 3rd Thailand Nanotechnology Conference. Bankok, pp. 52, 21–22.

Lai, M.H., Lee, M.W., Wang, G.-J., Tai, M.F., 2011. Photovoltaic performance of new-structure ZnO-nanorod dye sensitized solar cells. Int. J. Electrochem. Sci. 6, 2122–2130.

Loh, L., Dunn, S., 2012. Recent progress in ZnO-based nanostructured ceramics in solar cell applications. J. Nanosci. Nanotechnol. 12, 8215–8230.

Martinson, A.B.F., Elam, J.W., Hupp, J.T., Pellin, M.J., 2007. ZnO nanotube based dye-sensitized solar cells. Nano. Lett. 7, 2183–2187.

Matsui, M., Hashimoto, Y., Funabiki, K., Jin, J.-Y., Yoshida, T., Minoura, H., 2005. Application of near-infrared absorbing heptamethine cyanine dyes as sensitizers for zinc oxide solar cell. Synth. Met. 148, 147–153.

Noh, J.H., Lee, S.H., Lee, S., Jung, H.S., 2008. Influence of ZnO seed layers on charge transport in ZnO nanorod-based dye-sensitized solar cells. Electron. Mater. Lett. 4, 71–74.

Pugliese, D., Bella, F., Cauda, V., Lamberti, A., Sacco, A., et al, 2013. A chemometric approach for the sensitization procedure of ZnO flowerlike microstructures for dye-sensitized solar cells. ACS Appl. Mater. Interf. 5, 11288–11295.

Raksa, P., Nilphai, S., Gardchareon, A., Choopun, S., 2009. Copper oxide thin film and nanowires as a barrier in ZnO dye-sensitized solar cells. Thin Solid Films 517, 4741–4744.

Rao, A.R., Dutta, V., 2008. Achievement of 4.7% conversion efficiency on ZnO dye-sensitized solar cells fabricated by spray deposition using hydrothermally synthesized nanoparticles. Nanotechnology 19. Article number 445712.

Ribeiro, H.A., Sommeling, P.M., Kroon, J.M., Mendes, A., Costa, C.A.V., 2009. Dye-sensitized solar cells: novel concepts, materials, and state-of-the-art performances. Int. J. Green Energy 6, 245–256.

Teesetsopon, P., Kuma, S., Dutta, J., 2012. Photoelectrode optimization of zinc oxide nanoparticle based dye-sensitized solar cell by thermal treatment. Int. J. Electrochem. Sci. 7, 4988–4999.

Wang, Q., Moser, J., Graetzel, M., 2005. Electrochemical impedance spectroscopic analysis of dye-sensitized solar cells. J. Phys. Chem. B 109, 14945–14953.

Wu, J.-J., Chen, G.-R., Yang, H.-H., Ku, C.-H., Lai, J.-Y., 2007. Effects of dye adsorption on the electron transport properties in ZnO-nanowire dye-sensitized solar cells. Appl. Phys. Lett. 90, 213103–213109.

Xu, F., Dai, M., Lu, Y., Sun, L., 2010. Hierarchical ZnO nanowire-nanosheet architectures for high power conversion efficiency in dye-sensitized. J. Phys. Chem. C114, 2776–2782.

Yang, W., Wan, F., Chen, S., Jiang, C., 2009. Hydrothermal growth and application of ZnO nanowire films with ZnO and TiO_2 buffer layers in dye-sensitized solar cells. Nanoscale Res. Lett. 4, 1486–1492.

Yang, C.M., Hon, M.H., Leu, I.C., 2012. Hierarchical ZnO nanostructures growth by aqueous solution process for dye-sensitized solar cells. J. Electrochem. Soc. 159, H638–H643.